

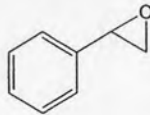
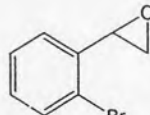
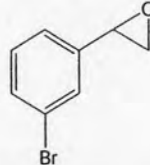
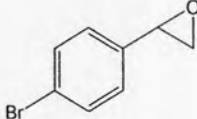
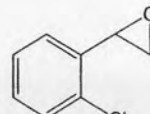
## CHAPTER III

### EXPERIMENTAL

#### 3.1 Epoxide derivatives

Most of the epoxide derivatives used in this study were obtained from the previous study of Yanchinda [16]. All aliphatic epoxide derivatives were purchased from Aldrich (purity 95-99%). The compound names, their abbreviations, and chemical structures of all relevant epoxide derivatives are given in Table 3.1.

**Table 3.1** Chemical structures and abbreviations of epoxide derivatives used for GC analysis.

Compound	Abbreviation	Chemical structure
styrene oxide	<b>1</b>	
<b>Group 1: styrene oxide derivatives with mono-substitution on aromatic ring</b>		
2-bromostyrene oxide	<b>2Br</b>	
3-bromostyrene oxide	<b>3Br</b>	
4-bromostyrene oxide	<b>4Br</b>	
2-chlorostyrene oxide	<b>2Cl</b>	

**Table 3.1** (continued)

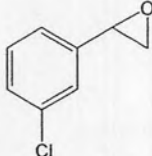
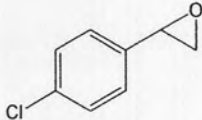
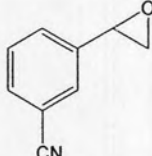
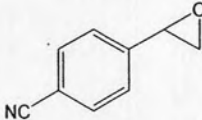
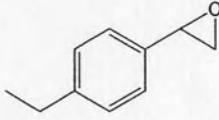
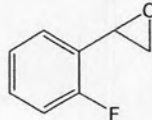
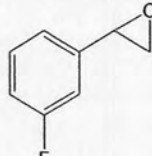
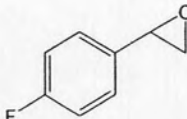
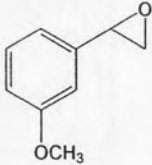
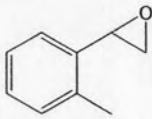
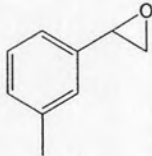
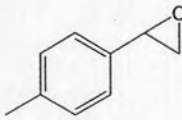
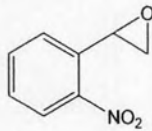
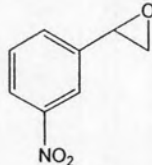
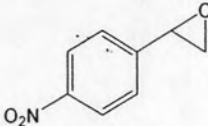
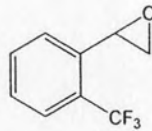
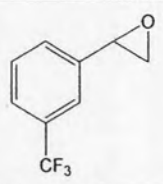
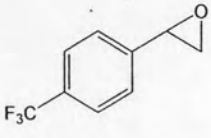
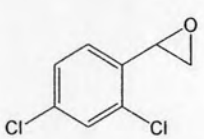
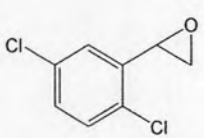
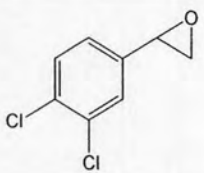
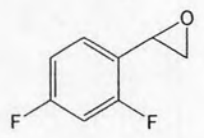
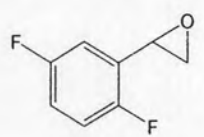
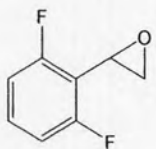
Compound	Abbreviation	Chemical structure
3-chlorostyrene oxide	<b>3Cl</b>	
4-chlorostyrene oxide	<b>4Cl</b>	
3-cyanostyrene oxide	<b>3CN</b>	
4-cyanostyrene oxide	<b>4CN</b>	
4-ethylstyrene oxide	<b>4Et</b>	
2-fluorostyrene oxide	<b>2F</b>	
3-fluorostyrene oxide	<b>3F</b>	
4-fluorostyrene oxide	<b>4F</b>	

Table 3.1 (continued)

Compound	Abbreviation	Chemical structure
3-methoxystyrene oxide	<b>3OMe</b>	
2-methylstyrene oxide	<b>2Me</b>	
3-methylstyrene oxide	<b>3Me</b>	
4-methylstyrene oxide	<b>4Me</b>	
2-nitrostyrene oxide	<b>2NO</b>	
3-nitrostyrene oxide	<b>3NO</b>	
4-nitrostyrene oxide	<b>4NO</b>	
2-(trifluoromethyl)styrene oxide	<b>2CF</b>	

**Table 3.1** (continued)

Compound	Abbreviation	Chemical structure
3-(trifluoromethyl)styrene oxide	<b>3CF</b>	
4-(trifluoromethyl)styrene oxide	<b>4CF</b>	
<b>Group 2: styrene oxide derivatives with di-substitution on aromatic ring</b>		
2,4-dichlorostyrene oxide	<b>24Cl</b>	
2,5-dichlorostyrene oxide	<b>25Cl</b>	
3,4-dichlorostyrene oxide	<b>34Cl</b>	
2,4-difluorostyrene oxide	<b>24F</b>	
2,5-difluorostyrene oxide	<b>25F</b>	
2,6-difluorostyrene oxide	<b>26F</b>	

**Table 3.1** (continued)

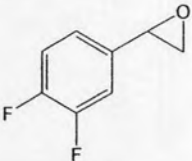
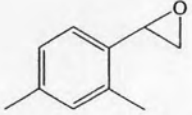
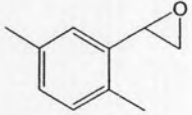
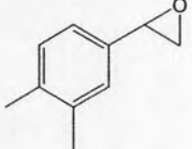
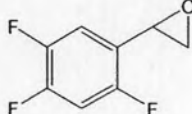
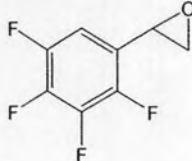
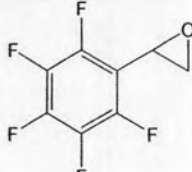
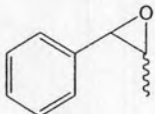
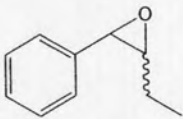
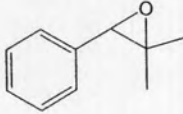
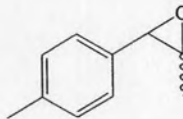
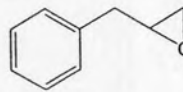
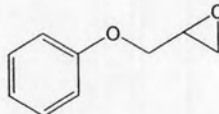
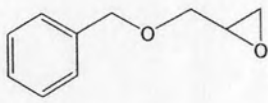

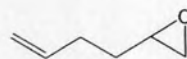
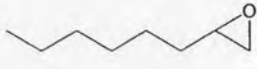
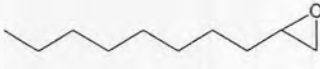
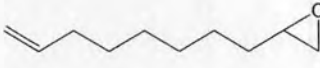
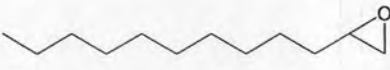
Compound	Abbreviation	Chemical structure
3,4-difluorostyrene oxide	<b>34F</b>	
2,4-dimethylstyrene oxide	<b>24Me</b>	
2,5-dimethylstyrene oxide	<b>25Me</b>	
3,4-dimethylstyrene oxide	<b>34Me</b>	
<b>Group 3: other aromatic epoxides</b>		
2,4,5-trifluorostyrene oxide	<b>triF</b>	
2,3,4,5-tetrafluorostyrene oxide	<b>tetraF</b>	
2,3,4,5,6-pentafluorostyrene oxide	<b>pentaF</b>	
phenylpropylene oxide	<b>2</b>	

Table 3.1 (continued)

Compound	Abbreviation	Chemical structure
phenylbutylene oxide	3	
phenylisopropylene oxide	4	
4-methylphenylpropylene oxide	5	
(2,3-epoxypropyl)benzene	6	
1,2-epoxy-3-phenoxypropane	7	
benzyl glycidyl ether	8	
<b>Group 4: aliphatic epoxides</b>		
1,2-epoxyhexane	hexa	
1,2-epoxy-5-hexene	5hexe	



**Table 3.1** (continued)

Compound	Abbreviation	Chemical structure
1,2-epoxyoctane	<b>octa</b>	
1,2-epoxydecane	<b>deca</b>	
1,2-epoxy-9-decene	<b>9dece</b>	
1,2-epoxydodecane	<b>dodec</b>	

### 3.2 Gas chromatographic analysis

All chromatographic analyses were performed on an Agilent 6890 series gas chromatograph equipped with a split/splitless injector and a flame ionization detector (FID). The temperature of injector and detector were maintained at 250 °C. Hydrogen was used as a carrier gas with an average linear velocity of 50 cm/s. The separation was carried out on the 15 m×0.25 mm i.d. capillary column coated with a 0.25 μm thick film of stationary phase. Three types of stationary phase were used in this research:

- polysiloxane OV-1701 (7% phenyl, 7% cyanopropyl, 86 % dimethylpolysiloxane, Supelco) as a reference stationary phase and a diluent for solid cyclodextrin derivatives in two chiral columns
- 32.8 % octakis(2,3-di-*O*-methyl-6-*O*-*tert*-butyldimethylsilyl) cyclomaltoooctaose (or GSiMe) in OV-1701

- 36.6 % octakis(2,3-di-*O*-acetyl-6-*O*-*tert*-butyldimethylsilyl) cyclomaltooctaose (or GSiAc) in OV-1701

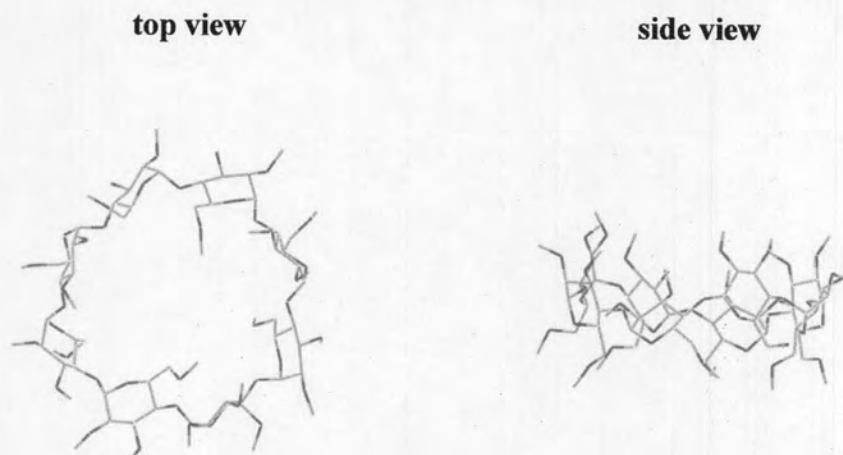
Two chiral columns were prepared to contain identical molality of cyclodextrin derivatives. All columns were conditioned at 200 °C until a stable baseline was observed. Each epoxide derivative was dissolved in hexane at a concentration of ~ 5–10 mg/mL. Approximately 0.2–0.5 µL of solution was injected at least in duplicate with a split ratio of 100:1. All thermodynamic studies were performed isothermally starting from 40 to 200 °C with 10 °C increments. Retention factors and enantioselectivities of all analytes were calculated from the chromatograms. Finally, thermodynamic parameters were determined by means of van't Hoff approach.

### 3.3 Details of molecular modeling

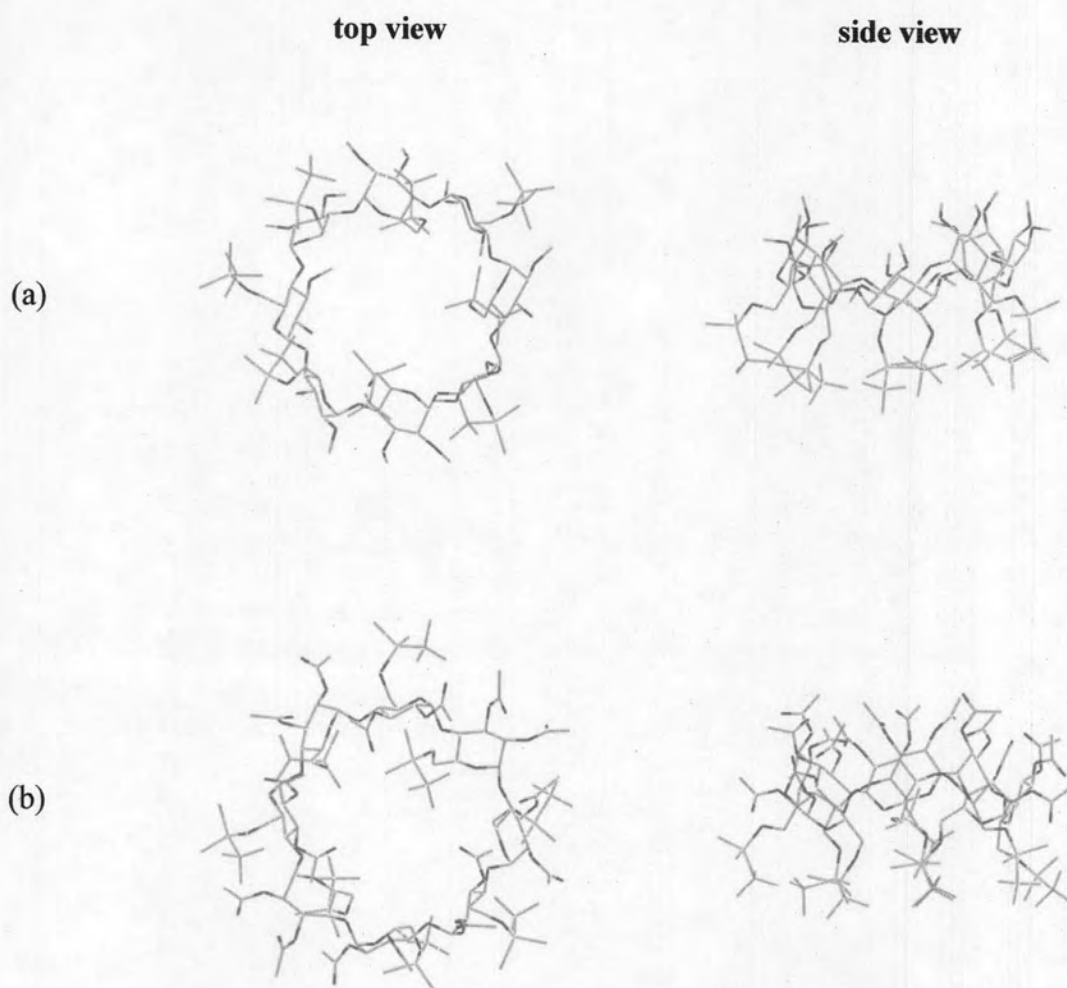
#### 3.3.1 Optimization of the host GSiMe and GSiAc

The starting atomic coordinates of GSiMe and GSiAc were taken from the X-ray crystal structure of permethylated  $\gamma$ -CD [40] (Figure 3.1); all H-atoms were omitted. All methyl C-atoms attached to O6 were replaced with *tert*-butyldimethylsilyl groups for GSiMe. All methyl C-atoms attached to O2, and O3 were replaced with acetyl groups and all methyl C-atoms attached to O6 were replaced with *tert*-butyldimethylsilyl groups for GSiAc. All H-atoms were added. The structures obtained were subsequently optimized with PM3 calculation using Gaussian03 [41] (Figure 3.2).





**Figure 3.1** X-ray crystal structure of the permethylated  $\gamma$ -cyclodextrin (C: gray; O: red) [40].



**Figure 3.2** PM3-optimized structures of (a) GSiMe and (b) GSiAc (C: gray; O: red; Si: yellow).

### 3.3.2 Optimization of the guest epoxides

All styrene oxide derivatives with mono-substitution on aromatic ring were selected as guests for the investigation of the chiral recognition with CD derivatives. The structures of both *R*- and *S*-forms were constructed by GaussView and were optimized at the HF/6-31G\*\* level using Gaussian03. The HF/6-31G\*\*-optimized structures were subsequently used for molecular docking calculations.

### 3.3.3 Molecular docking calculations

The molecular docking calculations were performed using the automated docking program, AutoDock 4.0.1 software [42]. The structure parameter files of host and guest molecules were prepared using AutoDockTools (ADT) [43]. Parameter files needed for docking calculation are defined as follows:

- Protein data bank file with partial charges and atom types (.pdbqt) is prepared from the initial pdb file by adding all hydrogens and partial charges and assignment the atom types were assigned to each atom of both the host and guest molecules.
- Grid parameter file (.gpf) is used to specify various parameters that AutoGrid uses to compute and create map file. The grid parameter file contains the following parameters:
  - the number of grid points in the x-, y-, and z- direction
  - the grid data field file name (.fld) to be created by AutoGrid
  - the spacing of each grid point
  - all atom types present in the host
  - all atom types present in the guest
  - the host molecule file name (.pdbqt)
  - the center of grid maps
  - file name of the grid map for all atom types of the guest (.map) to be created by AutoGrid

- file name for the electrostatic potential energy grid map (.map) to be created by AutoGrid
  - file name of the desolvation potential grid map (.map) to be created by AutoGrid
  - dielectric constant
- Docking parameter file (.dpf) is used to specify various parameters that are needed for AutoDock. The docking parameter file contains the following parameters:
- all atom types present in the guest
  - the grid data field filename (.fld)
  - file name of the grid map for all atom types in the guest (.map) to be created by AutoGrid
  - file name for the electrostatic potential energy grid map (.map) to be created by AutoGrid
  - file name of the desolvation potential grid map (.map) to be created by AutoGrid
  - file name for the guest to be docked
  - the center of the guest in a grid box
  - initial coordinates for the center of the guest or randomly set by users
  - number of rotatable bonds in the guest
  - initial relative dihedral angle
  - number of individuals in the populations
  - maximum number of energy evaluations
  - maximum number of generations
  - number of top individuals to survive for the next generation
  - rate of gene mutation
  - rate of crossover
  - etc.

The docking calculation procedures are briefly described as follows:

**Step 1:** Preparation of pdbqt file for guest molecule by adding all hydrogens, assigning partial charges and atom types to the guest molecule and setting either to an

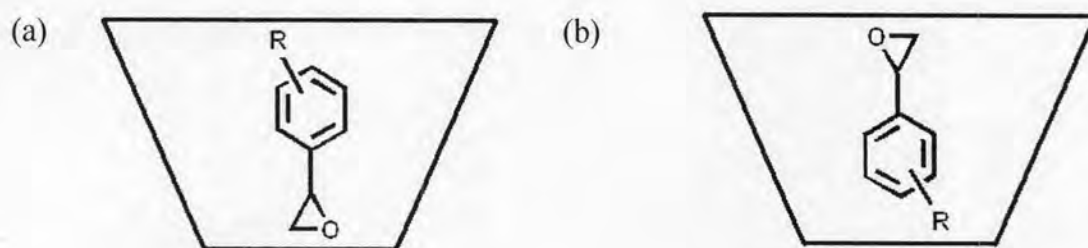
atom picked by the user or automatically to the atom which is considered to be in the center of the molecule (called as rigid root) and then set number of rotatable bonds in the guest molecule using the ADT.

**Step 2:** Preparation of pdbqt file for host molecule by adding all hydrogens and assigning partial charges and atom types to the host molecule.

**Step 3:** Preparation of grid parameter file. Grid box of dimension  $15 \times 15 \times 15 \text{ \AA}^3$  with a grid spacing of  $0.375 \text{ \AA}$  was used. The output was written as grid parameter file (gpf).

**Step 4:** Preparation of grid map file with AutoGrid to create map files for all atom types in the guest including electrostatic potential grid map and desolvation potential grid map.

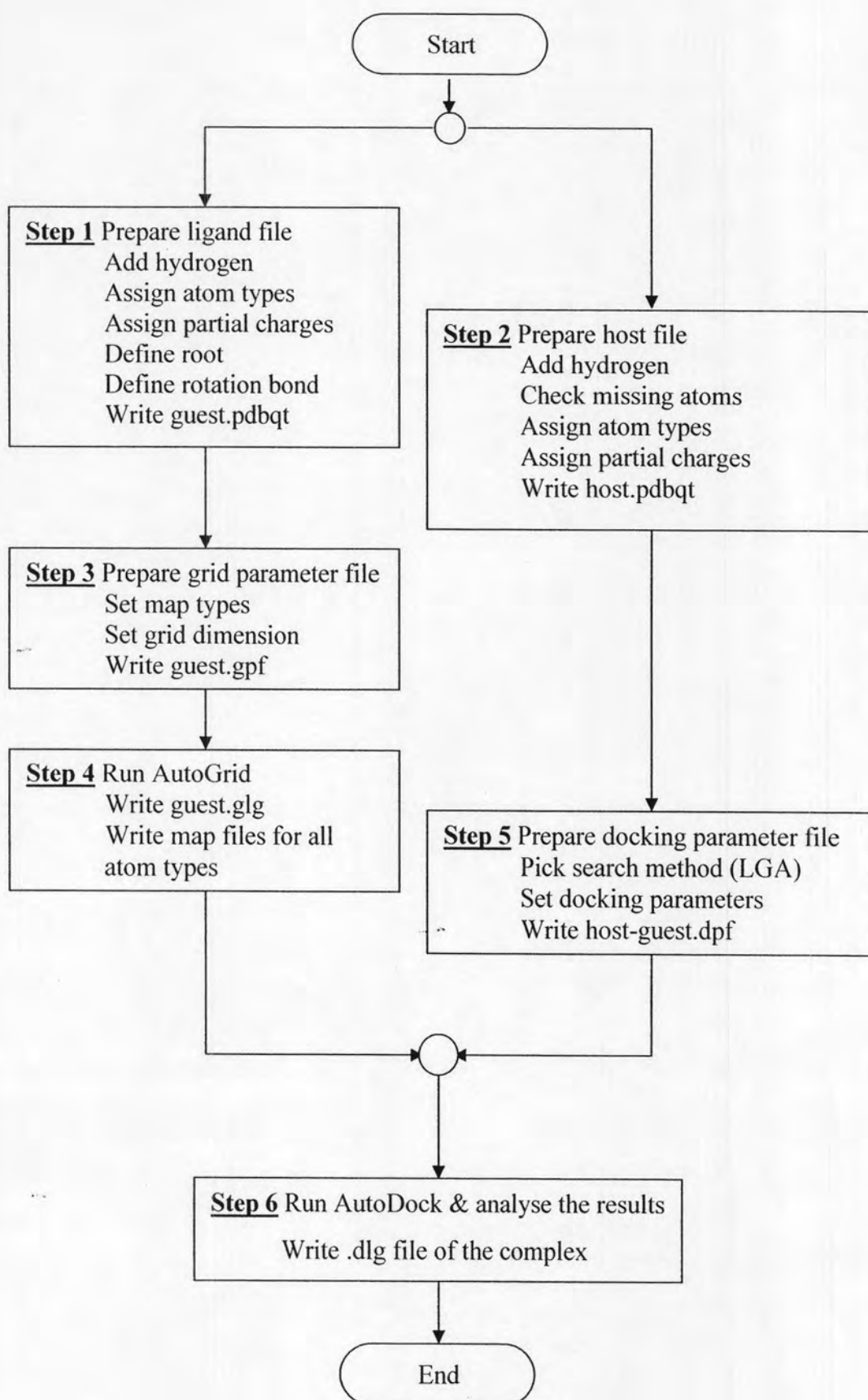
**Step 5:** Preparation of docking parameter file by using Lamarckian genetic algorithm (LGA) as the search algorithm. For the molecular docking calculations, 100 LGA runs with 300 numbers of individuals in the population were performed. The run was terminated if either 2,500,000 of energy evaluations or 27,000 numbers of generations were reached. The number of the top individuals in the current population that automatically survive into the next generation was set as 1. The rate of gene mutation and the rate of gene crossover were given as 0.02 and 0.80, respectively. Other parameters were set as default using ADT. Since the LGA is based on random movements, in order to avoid any bias, two possible orientations in the host CD cavity that epoxide group pointing toward primary side (down) and secondary side (up) were used as starting configurations in the docking calculation of each enantiomer (Figure 3.3). The output file was written as docking parameter file (dpf).



**Figure 3.3** Schematic representation of (a) down and (b) up orientations used as starting configurations in docking calculation.

**Step 6:** Run AutoDock & analyse the docking results from the docking log file (.dlg). The message "autodock4: Successful Completion" is found at the end of the file after the calculation is finished. The docking log file contains Cartesian atomic coordinates of the docked configuration and binding energy of each run. Configurations with root-mean-square-deviation (rmsd)  $\leq 1 \text{ \AA}$  were grouped together. In each group, the lowest binding energy configuration was selected as the representative of that group. The frequency represented the number of configuration in each group. Our attention was focused on the group with the highest frequency or the dominating configuration. The binding free energy difference of two enantiomers will be compared with that obtained from GC experiment. Because the binding free energy differences between the complexes of the two enantiomers obtained from AutoDock were found insignificant, the atomic coordinates of the highest frequency or the dominating docking configurations were re-optimized using PM3 method implemented in Gaussian03 to obtain the greater differences of binding energy. The flow chart showing the docking procedure with AutoDock is given in Figure 3.4.





**Figure 3.4** Flowchart illustrating the various steps of molecular docking using AutoDock.



### 3.3.4 Binding energy by PM3 calculation

Binding energy of the complex can be calculated from equation (27).

$$\Delta E_{\text{binding}} = E_{\text{complex}} - (E_{\text{host}} + E_{\text{guest}}) \quad (\text{kcal/mol}) \quad (27)$$

where  $\Delta E_{\text{binding}}$  is binding energy of the complex;

$E_{\text{complex}}$ ,  $E_{\text{host}}$  and  $E_{\text{guest}}$  are the formation energies of the complex, free host, and free guest, respectively.

The difference in calculated binding energy from PM3 method ( $\Delta\Delta E_{\text{PM3}}$ ) and the difference in GC-derived enthalpy change ( $\Delta\Delta H_{\text{GC}}$ ) of each enantiomeric complex cannot be directly compared because they are obtained from different conditions. The theoretical models of the complexes in the implicit solvent provide binding free energy ( $\Delta G_{\text{AutoDock}}$ ) of the isolated complex at 298 K, whereas GC provides enthalpy and entropy changes ( $\Delta H_{\text{GC}}$  and  $\Delta S_{\text{GC}}$ ) of the isolated guest included in the liquid host that is directly influenced by the experimental conditions (e.g. solvent, temperature, ionic strength, etc.). However, the tendency  $\Delta\Delta E_{\text{PM3}}$  and  $\Delta\Delta H_{\text{GC}}$  of various enantiomeric complexes can be compared and  $\Delta\Delta G_{\text{GC}}$  at 298 K can also be calculated.